



A99-16502

AIAA 99-0636

**The Effects of Icing on the Longitudinal
Dynamics of an Icing Research Aircraft**

**R. Miller and W. Ribbens
The University of Michigan
Ann Arbor, MI**

**37th AIAA Aerospace Sciences
Meeting and Exhibit
January 11-14, 1999 / Reno, NV**

THE EFFECTS OF ICING ON THE LONGITUDINAL DYNAMICS OF AN ICING RESEARCH AIRCRAFT

Robert H. Miller *
William B. Ribbens,

Department of Aerospace Engineering,
The University of Michigan, Ann Arbor, MI 48109 †

Abstract

Icing affects the aerodynamic performance of aircraft leading sometimes resulting in catastrophic crashes. The effects of icing have been studied in the past but from more of an aerodynamicist's viewpoint than a flight controls viewpoint. This paper develops models for aircraft dynamics in the presence of icing that can ultimately lead to a model based method of detecting icing. Flight test data from the NASA Lewis Twin Otter Icing Research Aircraft is analyzed in both case of a nominal un-iced configuration and a horizontal stabilizer experiencing icing due to a failed de-icing boot. Robust global nonlinear models were developed for each flap setting. The global nonlinear and localized linear models were analyzed for the differences between nominal and iced conditions with excellent agreement between model predictions and flight test data.

Introduction

Icing affects the aerodynamic performance of aircraft by contaminating the aerodynamic surfaces. Without anti-icing equipment icing, if sufficiently severe, can relatively quickly lead to a situation in which controllable flight is impossible. Even aircraft with anti-icing equipment are potentially susceptible to icing under certain conditions. Some turboprop aircraft that have de-icing boots on the leading edge of aerodynamic surfaces may experience wing and tailplane icing behind the de-icing boots. Moreover, de-icing boots can fail due to a variety of conditions including holes produced by rocks etc. In particular

the failure of a horizontal stabilizer boot can occur under such circumstances that the flight crew is unaware of the failure.

The goal of the present paper is to develop robust global nonlinear models for aircraft dynamics under tailplane icing scenarios. A longer term goal, that is presented in a related paper [1] is to use these models to detect icing via the associated changes in aircraft dynamics and though changes in control effectiveness. In this paper robust nonlinear models are developed from flight test data collected while flying a suitably instrumented aircraft that as had modifications made to aerodynamic surfaces simulating actual icing. The models themselves are sufficiently robust to include a wide range of flight conditions and in various configurations. In particular we present models that represent approach and landing configurations with simulated icing (due e.g to failed boot) on the horizontal stabilizer. In addition these models are valid for the full range of flap deflections (in e.g. landing configuration) for which stable controllable flight is possible. This is particularly significant for horizontal stabilizer icing since the tail stall margin is greatly reduced due to downwash induced by the flap deflection. Specifically the test aircraft used to obtain the models experienced almost complete loss of pitch control with flaps at 40°. Clearly it would benefit flight safety to be able to warn the pilot of such a condition.

The application of the models developed in this paper [1] is to continuously estimate elevator effectiveness via a state estimator that is driven by existing aircraft sensors as inputs. In the case of a failed horizontal stabilizer boot the loss of elevator effectiveness has been shown to be predictable as ice accretes. The algorithm used to predict the loss of effectiveness are highly computational efficient such that warnings to the pilot can be initiated well be-

*Supported in part by NASA under grant NGT4-52404

†Copyright ©1999 by Robert H. Miller Published by the American Institute of Aeronautics and Astronautics, Inc. with permission.

fore pitch control is lost.

The data set used to obtain the models presented was generously provided by NASA Lewis Research Center. The software packages, the Stepwise Regression, SWR[2], software package and Orthogonal Function Fit, OFFIT[3], software package, used to build the models were provided by NASA Langley Research Center. Funding for the research was provided by NASA Dryden Research Center.

This paper demonstrates the excellent fit of the model with the actual flight data. The models are quite robust to operating conditions including flight at 4 different flap settings and with and without ice. In addition, this paper shows that there is a significant trim change between the uniced and iced horizontal stabilizer. Such a trim change can provide one part of a method for detecting horizontal stabilizer icing.

Flight Test

The NASA Lewis twin otter Icing Research Aircraft was used to conduct flight tests with different cases of tailplane icing. Various shapes were attached to the horizontal stabilizer of the twin otter to simulate different levels of tailplane icing. These simulated icing attachments were developed from actual ice accumulation in the NASA icing research wind tunnel.

Aircraft weight and balance were based on previous weight and balance information, [4], and computations to take into account the changes since the previous flight tests. In flight measurements of the fuel usage were used to compute the center of gravity and moments of inertia for post flight data processing.

The maneuvers were performed in a decoupled manner which allowed the longitudinal subset of the dynamics to be separated out. The control input was a classic elevator doublet. The power control was maintained at a nearly constant combined thrust coefficient of about $C_T = 0.1$, yielding a thrust of approximately 1000lbf. Each maneuver last approximately 12 to 14 seconds. An example of the input is shown in Figure 1.

There were two distinct flight test configurations analyzed. The different cases are shown in Table 2. The un-iced configuration represents the nominal aircraft. The failed boot configuration represents the level of icing 22 minutes after a de-icing boot fails on an aircraft experiencing icing. The 22 minutes is derived from a FAA requirement.

Results

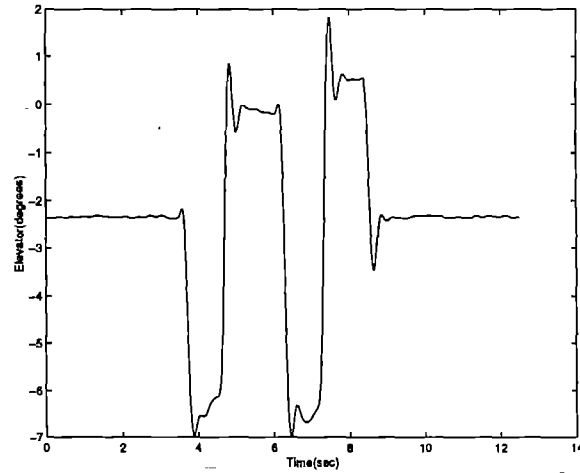


Figure 1: Typical Elevator Input for Flight Tests

Table 1		
Flight Test Maneuvers		
Configuration	Maneuver	δ_F (Flap Angle)
Failed Boot	p46	0,10,20,30
Nominal	p52	0,10,20,30

The following body axis equations, [5], were used to model the longitudinal dynamics of the twin otter icing research aircraft.

$$\dot{X} = f(X, V) \quad (1)$$

$$\begin{bmatrix} \dot{u} \\ \dot{w} \\ \dot{\theta} \\ \dot{q} \end{bmatrix} = \begin{bmatrix} -wq + \frac{F_x}{m} - g_x \\ uq + \frac{F_z}{m} + g_z \\ q \\ \bar{q}ScC_m/I_y \end{bmatrix} \quad (2)$$

$$\begin{aligned} \bar{q} &= \frac{1}{2}\rho(u^2 + w^2) & \alpha &= \tan^{-1}\left(\frac{w}{u}\right) \\ F_x &= \bar{q}SC_x + T_x, & F_z &= \bar{q}SC_z + T_z \\ g_x &= \sin(\theta)g, & g_z &= \cos(\theta)g. \end{aligned}$$

where C_x, C_z , and C_m are polynomial functions of α , q , and δ_e (note the q is dimensional and not the typical nondimensional). A more detailed explanation of the variables is in the Appendix. The functions for the SWR cases are of the form,

$$C_x = x_1\alpha + x_2\alpha^2 + x_3\delta_e + x_4 \quad (3)$$

$$C_z = z_1\alpha + z_2q + z_3\alpha^2 + z_4\delta_e + z_5 \quad (4)$$

$$C_m = m_1\alpha + m_2q + m_3\alpha^2 + m_4\delta_e + m_5 \quad (5)$$

The results of the SWR fit and the OFFIT fit are listed in the tables in the Appendix. The OFFIT

polynomials are also described in detail in the Appendix. An example of the fit for C_z is shown in Figures 2 and 3.

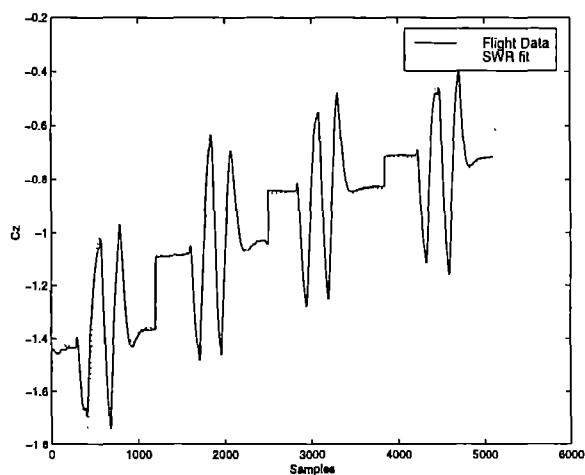


Figure 2: SWR Fit of C_z

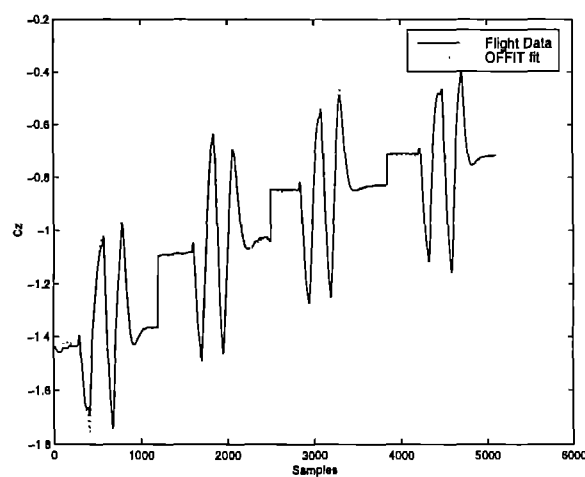


Figure 3: OFFIT Fit of C_z

Comparisons of open loop simulations of the SWR fitted polynomial functions versus the actual flight data for angle of attack are shown in Figure 4 and Figure 5. The pitch rate responses are shown in Figure 6 and Figure 7. The robustness of the polynomial fits discussed above is reflected in the excellent fit of the dynamic α and q for both the nominal and failed boot cases. These two variables play an important role in the model based ice detection scheme presented in [1]. In particular the pitch rate fit for both nominal and failed boot case is important when estimating elevator effectiveness.

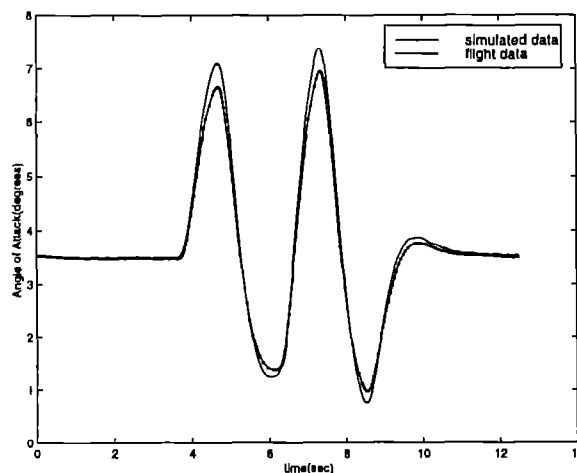


Figure 4: Nominal Angle of Attack α

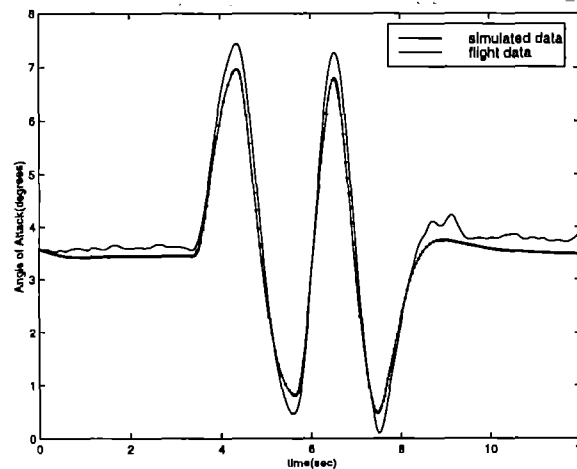


Figure 5: Failed Boot Angle of Attack α

Figure 8 shows the elevator trim change between the uniced and iced horizontal stabilizer at flaps 0° , 10° , 20° , and 30° . The flight conditions for these flap settings were the same (as much as is practically significant) for iced and uniced conditions. This change has the potential to provide one element of an ice detection method. For example in an aircraft flying on autopilot in icing conditions the elevator/trim tab setting could be monitored. The indicated change could, for example, set a software flag that in combination with the state estimator output explained in the related paper, [1], could be used to detect a loss of elevator effectiveness.

Acknowledgements

The authors would like to thank Thomas Ratvasky

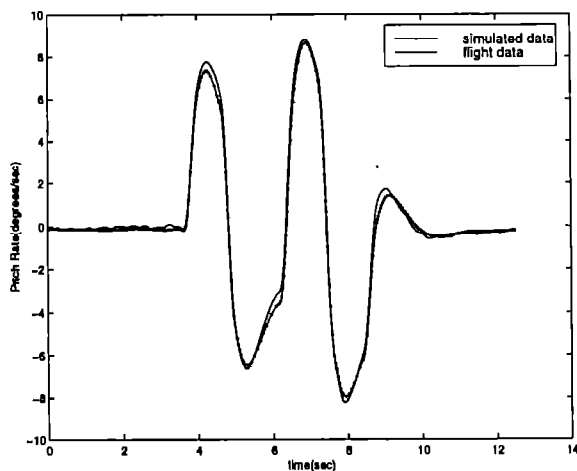
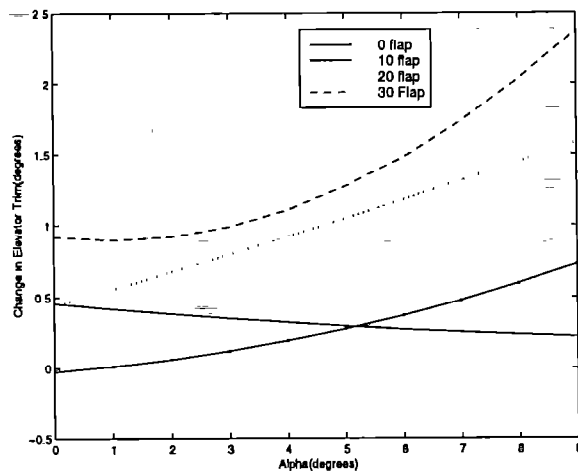
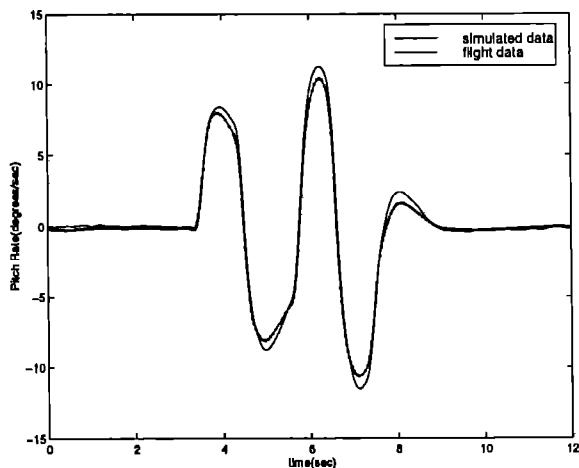
Figure 6: Nominal Pitch Rate q 

Figure 8: Elevator Trim Change

Figure 7: Failed Boot Pitch Rate q

of NASA Lewis Research Center and Judith Van Zante of NYMA, Inc., for their helpful discussions and comments. The flight test data was generously supplied by NASA Lewis Research Center. Also Dr. Gene Morelli of NASA Langley provided assistance with the SWR, stepwise regression, and the OFFIT, orthogonal function, flight test data fitting code from NASA Langley as well as some helpful comments.

References

- [1] Robert H. Miller and William B. Ribbens. Detection of the Loss of Elevator Effectiveness due to Icing. Number 99-0637 in 37th Aerospace Sciences. AIAA, Jan. 1999.
- [2] Vladislav Klein, James G. Batterson, and Patrick C. Murphy. Determination of Airplane Model Structure from Flight Data using Modified Stepwise Regression. Technical Report 1916, NASA, 1981.
- [3] Eugene A. Morelli. Global Nonlinear Aerodynamic Modeling Using Multivariate Orthogonal Functions. *Journal of Aircraft*, 32(2):270-277, March-April 1995.
- [4] T.P. Ratvasky and R.J. Ranaudo. Icing Effects on the Aircraft Stability and Control Determined from Flight Data. Technical Report 105977, NASA, 1993.
- [5] John H. Blakelock. *Automatic Control of Aircraft and Missiles*. John Wiley, 2nd edition edition, 1991.

Appendix Equations of Motion

$$\dot{X} = f(X, V) \quad (6)$$

$$\begin{bmatrix} \dot{u} \\ \dot{w} \\ \dot{\theta} \\ \dot{q} \end{bmatrix} = \begin{bmatrix} -wq + \frac{F_x}{m} - g_x \\ uq + \frac{F_z}{m} + g_z \\ q \\ \bar{q}ScC_m/I_y \end{bmatrix} \quad (7)$$

$$\begin{aligned} \bar{q} &= \frac{1}{2}\rho(u^2 + w^2) & \alpha &= \tan^{-1}\left(\frac{w}{u}\right) \\ F_x &= \bar{q}SC_x + T_x, & F_z &= \bar{q}SC_z + T_z \\ g_x &= \sin(\theta)g, & g_z &= \cos(\theta)g. \end{aligned}$$

Where u is the longitudinal speed in body axes and w is the vertical speed in body axes. θ is the pitch angle and q is the pitch angle rate. v is the elevator angle, δ_e . g is gravity. \bar{q} is the dynamic pressure. S is the wing area, $39.02m$, and c is the wing mean chord, $1.98m$. The components of thrust along the body x and z coordinates are denoted T_x and T_z respectively and are $T_x = 4864N$ and $T_z = 212N$.

Appendix SWR FitAppendix OFFIT Fit

The OFFIT attempts to build a global aerodynamic model from flight data using multivariate orthogonal functions, [3]. The following tables contain the results of the offit fit. The aerodynamic coefficients are function based on the following variables,

$$C_x(\alpha, \delta_e) \quad (8)$$

$$C_z(\alpha, q, \delta_e) \quad (9)$$

$$C_m(\alpha, q, \delta_e) \quad (10)$$

The structure of each polynomial is of the form

$$C_n(\bullet) = \sum_{i=1}^I n_i \prod_{j=1}^J \nu_{nj}^{i_j} \quad n = x, z, m \quad (11)$$

where n_i is the i th coefficient and ν_{nj} = j th independent variable in C_n . For example Table 1 lists the coefficients for the functions in equations 8, 9, and 10 for zero flaps. The function C_x is a function of two variables (ie $J = 2$, $\nu_{x1} = \alpha$, $\nu_{x2} = \delta_e$). There are 8 terms in this polynomial with coefficients x_i ($i = 1, \dots, 8$). The index column lists the exponent of each variable in sequence. An example of the a fit would be C_x for the 0° flap setting case.

$$\begin{aligned} C_x(\alpha, \delta_e) &= -0.071 + 0.303\alpha + 0.157\delta_e + 3.281\alpha^2 \\ &\quad -1.788\alpha\delta_e - 0.902\delta_e^2 + 10.054\delta_e\alpha^2 + 7.082\delta_e^2\alpha \end{aligned} \quad (12)$$

SWR FIT C_x				
$\delta_F = 0$				
	x_1	x_2	x_3	x_4
p52	0.3900	2.9099	0.0961	-0.0758
σ_x	0.0728	0.2987	0.0162	0.0041
p46	0.714	1.7440	0.0682	-0.0896
σ_x	0.0894	0.3419	0.0155	0.0052
$\delta_F = 10$				
p52	0.3364	4.4990	0.1174	-0.1149
σ_x	0.0259	0.2501	0.0166	0.0012
p46	0.3869	5.0679	0.1072	-0.1178
σ_x	0.0228	0.1933	0.0114	0.0010
$\delta_F = 20$				
p52	0.3302	5.3376	0.2002	-0.2055
σ_x	0.0579	0.4078	0.0340	0.0031
p46	0.5175	5.4043	0.1710	-0.1982
σ_x	0.0352	0.2557	0.0231	0.0023
$\delta_F = 30$				
p52	0.3357	5.7471	0.2438	-0.3096
σ_x	0.0962	0.7143	0.0753	0.0054
p46	0.5010	6.1872	0.2184	-0.2967
σ_x	0.0738	0.5936	0.0505	0.0050

SWR FIT C_z					
$\delta_F = 0$					
	z_1	z_2	z_3	z_4	z_5
p52	-7.0186	-0.1023	4.1109	-0.2340	-0.3112
σ_z	0.2219	0.0356	0.8616	0.0500	0.0121
p46	-7.5095	-0.2375	6.5731	-0.3541	-0.3175
σ_z	0.3491	0.0493	1.3377	0.0599	0.0208
$\delta_F = 10$					
p52	-7.1429	0.2738	0.6482	0.0338	-0.9135
σ_z	0.0630	0.0365	0.7213	0.0486	0.0027
p46	-7.4225	0.3008	1.9348	0.0467	-0.9366
σ_z	0.0782	0.0398	0.7689	0.0502	0.0034
$\delta_F = 20$					
p52	-7.7552	0.4784	4.5098	0.0611	-1.4455
σ_z	0.0758	0.0482	0.6768	0.0485	0.0037
p46	-7.8163	0.6433	5.0107	0.3061	-1.4858
σ_z	0.0656	0.0483	0.5686	0.0507	0.0049
$\delta_F = 30$					
p52	-8.1446	0.7462	5.4151	0.1159	-1.8940
σ_z	0.0890	0.0778	1.1494	0.0697	0.0066
p46	-8.2405	0.9358	5.3024	0.2610	-1.8698
σ_z	0.0505	0.0477	0.6017	0.0403	0.0034

SWR FIT C_m					
$\delta_F = 0$					
	z_1	z_2	z_3	z_4	z_5
p52	-0.8789	-0.6266	-3.8520	-1.8987	-0.0108
σ_m	0.0966	0.0180	0.3909	0.0252	0.0055
p46	-0.7899	-0.6899	-3.9300	-1.8629	-0.0255
σ_m	0.1632	0.0206	0.6332	0.0273	0.0102
$\delta_F = 10$					
p52	-1.2885	-0.5672	-3.0061	-1.7991	0.0836
σ_m	0.0347	0.0203	0.4118	0.0276	0.0015
p46	-1.2143	-0.5047	-3.2362	-1.6219	0.0761
σ_m	0.0441	0.0223	0.4543	0.0286	0.0018
$\delta_F = 20$					
p52	-1.5091	-0.6352	-1.9476	-1.7448	0.0654
σ_m	0.0289	0.0203	0.2651	0.0203	0.0013
p46	-1.3633	-0.4217	-1.6774	-1.3937	0.0415
σ_m	0.0345	0.0255	0.3568	0.0267	0.0027
$\delta_F = 30$					
p52	-1.8661	-0.6122	-2.1288	-1.6955	0.0274
σ_m	0.0352	0.0315	0.3836	0.0292	0.0019
p46	-1.3497	-0.4467	-3.2938	-1.2787	0.0002
σ_m	0.0467	0.0388	0.5609	0.0340	0.0035

OFFFIT FIT					
$\delta_F = 0$					
Nominal(p52)			Failed Boot(p46)		
x_i	σ_{x_i}	index	x_i	σ_{x_i}	index
-0.071	0.005	0	-0.084	0.006	0
0.303	0.091	1	0.582	0.103	1
0.157	0.087	10	0.066	0.095	10
3.281	0.424	2	2.442	0.442	2
-1.788	0.866	11	-1.090	0.940	11
-0.902	0.609	20	-0.849	0.488	20
10.054	4.148	12	8.953	3.677	12
7.082	4.118	21	6.882	3.462	21
z_i	σ_{z_i}	index	z_i	σ_{z_i}	index
-0.373	0.012	0	-0.359	0.016	0
-5.766	0.226	1	-6.346	0.269	1
-0.446	0.127	10	-0.292	0.127	10
-1.262	0.149	100	-0.924	0.163	100
-1.831	1.031	2	0.141	1.116	2
11.484	2.121	11	9.815	2.034	11
18.459	2.310	101	13.124	2.376	101
0.751	0.277	20	0.615	0.226	20
0.215	0.389	110	0.529	0.335	110
-0.313	0.362	200	-0.236	0.260	200
-62.875	8.664	12	-63.167	8.404	12
-78.176	9.271	102	-63.473	9.189	102
m_i	σ_{m_i}	index	m_i	σ_{m_i}	index
-0.023	0.008	0	0.008	0.009	0
-0.636	0.135	1	-1.097	0.130	1
-0.814	0.127	10	-0.447	0.091	10
-2.175	0.170	100	-1.376	0.130	100
-4.985	0.597	2	-3.494	0.532	2
4.141	1.261	11	0.600	0.941	11
4.130	1.797	101	-2.875	1.253	101
-0.233	0.577	20	0.168	0.355	20
-1.747	1.573	110	1.414	0.770	110
-1.329	0.902	200	1.465	0.558	200
-13.475	4.325	12	-8.098	3.243	12
-7.729	5.908	102	3.765	4.574	102
11.221	3.585	21	5.307	2.318	21
6.688	9.516	111	-7.805	4.742	111
16.591	6.833	201	-3.517	3.838	201
2.800	2.792	120	-2.015	1.239	120
-14.266	3.332	210	-9.599	1.493	210

OFFFIT FIT					
$\delta_F = 10$					
Nominal(p52)			Failed -0.Boot(p46)		
x_i	σ_{x_i}	index	x_i	σ_{x_i}	index
-0.114	0.001	0	-0.117	0.001	0
0.291	0.026	1	0.356	0.023	1
0.127	0.023	10	0.120	0.015	10
4.715	0.266	2	5.204	0.200	2
0.307	0.414	11	0.305	0.301	11
-0.283	0.237	20	-0.315	0.149	20
-1.057	3.092	12	-2.977	2.246	12
7.050	3.083	21	4.789	1.934	21
z_i	σ_{z_i}	index	z_i	σ_{z_i}	index
-0.919	0.003	0	-0.943	0.003	0
-7.176	0.079	1	-7.418	0.063	1
0.365	0.040	10	0.370	0.040	10
0.157	0.065	100	0.198	0.054	100
1.823	0.674	2	3.280	0.672	2
0.668	0.690	11	-24.977	5.796	12
1.694	1.516	101	-41.215	7.105	102
-0.734	0.790	110			
-30.728	8.574	12			
-49.189	9.831	102			
m_i	σ_{m_i}	index	m_i	σ_{m_i}	index
0.081	0.001	0	0.072	0.002	0
-1.286	0.039	1	-1.186	0.042	1
-0.507	0.024	10	-0.440	0.024	10
-1.729	0.036	100	-1.535	0.031	100
-2.885	0.406	2	-3.156	0.435	2
0.452	0.334	11	0.299	0.371	11
-1.969	0.827	101	-2.776	0.791	101
0.192	0.263	20	0.335	0.243	20
1.274	0.442	110	1.398	0.366	110
-0.563	0.401	200	-0.485	0.306	200
-20.704	3.465	12	-18.827	3.735	12
-11.492	8.487	102	-4.492	8.295	102
8.409	3.991	21	3.178	3.386	21
-7.556	10.168	111	-14.888	9.437	111
12.488	7.062	201	12.666	6.067	201
7.493	3.667	120	2.332	3.336	120
-8.318	3.680	210	-13.337	2.583	210

OFFFIT FIT					
$\delta_F = 20$					
Nominal(p52)			Failed Boot(p46)		
x_i	σ_{x_i}	index	x_i	σ_{x_i}	index
-0.203	0.003	0	-0.198	0.002	0
0.253	0.060	1	0.462	0.035	1
0.217	0.037	10	0.189	0.024	10
5.749	0.431	2	5.793	0.258	2
1.066	0.643	11	0.831	0.330	11
-0.269	0.367	20	0.050	0.166	20
-4.887	4.313	12	-6.882	1.964	12
5.781	3.798	21			
z_i	σ_{z_i}	index	z_i	σ_{z_i}	index
-1.451	0.003	0	-1.496	0.003	0
-7.780	0.050	1	-7.934	0.057	1
0.598	0.048	10	0.843	0.046	10
0.225	0.049	100	0.325	0.051	100
4.591	0.423	2	4.466	0.478	2
0.223	0.609	110	-0.699	0.465	11
-28.396	4.779	12	0.038	0.871	101
-29.466	5.950	102	0.398	0.477	110
			1.360	0.426	200
			-42.356	4.597	12
			-46.515	6.530	102
			-3.375	5.534	21
			-52.218	9.612	111
			-28.646	4.687	201
			-16.088	4.076	120
			-32.768	3.759	210
m_i	σ_{m_i}	index	m_i	σ_{m_i}	index
0.062	0.002	0	0.034	0.002	0
-1.519	0.033	1	-1.325	0.027	1
-0.608	0.025	10	-0.384	0.026	10
-1.682	0.029	100	-1.310	0.025	100
-2.111	0.258	2	-2.827	0.246	2
1.096	0.248	11	-0.929	0.183	11
-0.273	0.551	101	-2.418	0.450	101
0.771	0.293	20	0.520	0.211	20
1.506	0.302	110	0.611	0.183	110
-0.148	0.316	200	-0.196	0.235	200
-12.850	2.306	12	-9.229	2.009	12
-7.698	4.380	102	-9.293	2.938	102
-1.315	3.125	21	-2.221	2.339	21
-18.908	6.337	111	-19.571	4.257	111
2.997	3.754	201	-3.938	2.170	201
-3.616	2.666	120	-5.311	1.696	120
-13.280	2.091	210	-13.998	1.700	210

OFFFIT FIT					
$\delta_F = 30$					
Nominal(p52)			Failed Boot(p46)		
x_i	σ_{x_i}	index	x_i	σ_{x_i}	index
-0.313	0.005	0	-0.296	0.005	0
0.231	0.092	1	0.444	0.072	1
0.325	0.071	10	0.302	0.055	10
6.740	0.853	2	6.247	0.638	2
0.651	0.987	11	0.434	0.674	11
0.167	0.547	20	-0.176	0.364	20
-15.720	6.606	12	-14.891	6.575	12
4.196	5.550	21	4.334	5.439	21
z_i	σ_{z_i}	index	z_i	σ_{z_i}	index
-1.903	0.007	0	-1.876	0.003	0
-7.970	0.088	1	-8.293	0.053	1
0.764	0.073	10	1.151	0.066	10
0.163	0.056	100	0.351	0.054	100
6.466	0.946	2	5.004	0.601	2
-6.984	0.811	11	-2.910	0.694	11
-6.421	1.312	101	-2.361	0.772	101
-0.829	0.759	20	-0.942	0.739	110
0.897	0.580	110	-51.461	7.991	12
0.343	0.604	200	-30.673	12.980	102
-22.968	6.700	12	4.119	10.278	21
-54.806	10.479	102	-30.820	20.595	111
4.096	9.706	21	3.111	8.237	201
48.554	12.299	111	-20.589	7.850	120
			-42.077	6.595	210
m_i	σ_{m_i}	index	m_i	σ_{m_i}	index
0.021	0.003	0	-0.003	0.003	0
-1.858	0.038	1	-1.307	0.035	1
-0.597	0.035	10	-0.468	0.034	10
-1.687	0.026	100	-1.238	0.032	100
-1.979	0.456	2	-4.575	0.386	2
-0.308	0.375	11	-1.877	0.402	11
-1.727	0.763	101	-4.338	0.542	101
1.033	0.411	20	0.488	0.275	20
1.893	0.273	110	0.417	0.314	110
0.184	0.306	200	-0.730	0.232	200
-10.323	3.263	12	-5.049	4.853	12
-10.383	4.934	102	-9.287	7.719	102
1.092	3.877	21	-20.504	5.872	21
-8.503	6.578	111	-11.693	10.779	111
4.788	3.677	201	-0.278	4.702	201
-5.922	2.951	120	-21.994	4.508	120
-15.882	2.492	210	-16.635	3.474	210